Controlled inhibition of spiking dynamics in VCSELs for neuromorphic photonics: theory and experiments

JOSHUA ROBERTSON,[1] TAO DENG,[1,2] JULIEN JAVALOYES,[3] ANTONIO HURTADO[1,*]

[1]*Institute of Photonics, SUPA Department of Physics, University of Strathclyde, TIC Centre, 99 George Street, Glasgow, G1 1RD, United Kingdom*
[2]*School of Physical Science and Technology, Southwest University, Chongqing, 400715, China*
[3]*Departament de Fisica, Universitat de les Illes Balears, c/Valldemossa km 7.5, 07122, Mallorca, Spain*
**Corresponding author: antonio.hurtado@strath.ac.uk*

Received XX Month XXXX; revised XX Month, XXXX; accepted XX Month XXXX; posted XX Month XXXX (Doc. ID XXXXX); published XX Month XXXX

We report experimentally and on theory on the controllable inhibition of spiking regimes in a 1300 nm wavelength Vertical Cavity Surface Emitting Laser (VCSEL). Reproducible suppression of spiking dynamics is demonstrated at fast operation speeds (up to sub-ns rates) and with total control on the temporal duration of the spiking inhibition windows. This work opens new paths towards photonic inhibitory neuronal model system for use in future neuromorphic photonic information processing modules and which are able to operate at speeds up to 8 orders of magnitude faster than biological neurons. © 2017 Optical Society of America

OCIS codes: *(140.5960) Semiconductor Lasers; (140.7260) Vertical Cavity Surface Emitting Lasers; (200.4700) Optical Neural Systems;*

http://dx.doi.org/10.1364/OL.99.099999

Neuronal models for new paradigms in computing have been researched for decades [1]. Traditionally, electronic techniques have been mainly used for neuromorphic systems yielding already platforms such as Neurogrid at Stanford [2], TrueNorth at IBM [3], HICANN at the University of Heidelberg [4] and the University of Manchester's neuromorphic chip [5]. Electronic techniques however face important challenges, e.g. limited bandwidth, large multicasting and communication issues, which ultimately impose performance limits [6]. Photonic approaches for neuronal models have recently emerged as they can yield ultrafast operation speeds (up to 9 orders of magnitude faster than biological neurons) and offer high prospects for high integration and scalability, reduced crosstalk and large communication links (for a review see [6]).

However, whilst isolated works appeared as early as in year 2000 [7-9] it is only recently that the field has exploded [6-33] and diverse photonic neuronal models have been proposed using semiconductor optical amplifiers [10-12], fibre lasers [13-16], photonic crystal cavities [17,18], laser-photodiode coupled systems [19,20], semiconductor lasers (SLs) [21-34], etc. Of all these, SL approaches have attracted higher interest, since SLs can undergo behaviours analogous to those of neurons, such as excitability [34-36] and complex dynamics [37][38] but at timescales 7 to 9 orders of magnitude faster. Different types of SLs have been reported for photonic neuronal models, e.g. micro-ring [21], quantum-dot [34], two-section [6][22], micro-pillar [23][24] and vertical-cavity surface-emitting lasers (VCSELs) [26-31]. Practical applications have also been outlined in parallel information processing [6][22][32], pattern formation [6][30][33] and recognition [6][11], memory operation [20][29], etc. These features added to their compactness, potentials for on-chip integration and scalability into networks and compatibility with optical communication technologies [39] ensure that SLs will play a key role in future neuromorphic information processing systems [6].

Amongst SLs, VCSELs offer unique advantages, e.g. reduced manufacturing costs and energy consumption, easy integration in 2D/3D arrays, etc. [40][41], making them ideal for photonic neuronal models and networks. In spite of this, VCSELs have only recently started to be investigated for photonic neurons [26-31]. Emulation of neuronal responses using the polarization switching (PS) [26], nonlinear dynamics [27] and excitability [28-30] responses induced in VCSELs under optical injection has been reported. Also, controllable firing of sub-ns spikes [28-30], and diverse spike firing patterns [30] have been recently reported in VCSELs and their use for all-optical memory applications has been suggested [29].

Nonetheless, to date the majority of works focused on emulating excitatory neurons (which fire spikes when stimulated) by producing spiking regimes with SLs. Yet, neurons are fascinating systems yielding a wide range of computational responses depending on their type and nature of the arriving stimuli [43-45]. Another behavior in neurons is spike inhibition, where the arrival of a stimulus stops spiking activity [43-45]. In fact, inhibitory neurons in the brain play a key role to generate the signals stopping spiking activity and also to create order in neuronal networks by counteracting excitatory forces with opposed inhibitory ones

[43-45]. Moreover, inhibitory response is also important in the learning rules based upon spike-timing-dependent plasticity (STDP) [12]. Hence, future neuromorphic photonic networks aiming at emulating the powerful brain computational capabilities, will require the development of inhibitory photonic neuronal models.

This work demonstrates a VCSEL-based inhibitory photonic neuronal model. Controllable and reproducible inhibition of spiking dynamics is achieved at speeds up to 8 orders of magnitude faster than neurons (sub-ns rates) and with low power requirements (~tens of μWs). Numerical modeling also shows very good agreement with the experiments. Importantly, our approach uses inexpensive devices working at telecom wavelengths (1300 nm). These results offer high potentials for the use of VCSELs as a single platform for excitatory [30] and inhibitory neuronal models for future neuromorphic photonic systems.

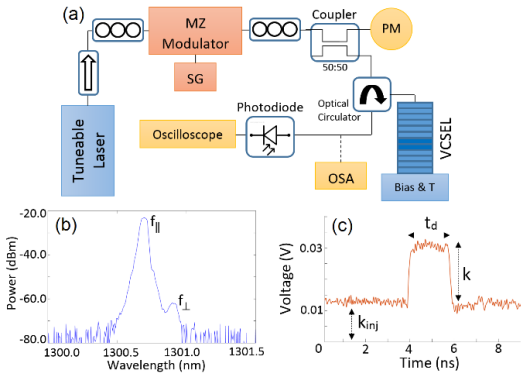

Fig. 1 (a) Experimental setup. (b) Spectrum of the VCSEL (I_{Bias} = 3mA). (c) Input signal with an added perturbation. MZ=Mach-Zehnder, SG=Signal Generator, OSA=Optical Spectrum Analyser.

Fig. 1(a) plots the experimental setup. Linearly polarized light from a 1300 nm tuneable laser (Master Laser, ML, HP81678) is injected into a commercially-available and fibre-pigtailed 1300 nm VCSEL from Raycan [46]. The latter, was set at 293 K and had a threshold current of 0.69 mA. The VCSEL's spectrum in fig. 1(b) shows emission at 1300.7 nm (at 3mA) with two peaks corresponding to the two orthogonal polarizations of the fundamental transverse mode. Throughout this work we refer to the polarisation of the main lasing (subsidiary) mode of the VCSEL as parallel (orthogonal) polarisation. Optical signals with added perturbations were injected into the VCSEL. These were generated modulating the ML's output with a Mach Zehnder (MZ) modulator (JDSU MOD-9189) and a signal generator allowing the generation of pulses with variable durations (from 0.2 to 10ns) and repetition rates (up to 15MHz). Fig. 1(c) plots a typically injected signal with a constant intensity level (k_{inj}) and perturbations in the form of positive pulses with defined duration (t_d), strength (k) and repetition rate (f_{rep} =15 MHz). k_p is defined as the ratio between the pulse intensity and the constant injection level ($k_p = k/k_{inj}$). Here, we present results obtained when the signals from the ML are set with orthogonal polarization and are injected into the orthogonal polarization mode of the VCSEL. Finally, the VCSEL's output was analyzed with an Optical Spectrum Analyzer and with a 9.5GHz amplified photodetector (Thorlabs PDA8GS) and a 13 GHz real time oscilloscope.

Fig. 2(a) shows time series at the VCSEL's output under the injection of the signal in fig. 2(b). The latter had a power of $k_{inj} = 33.56\ \mu W$ and a frequency detuning (Δf), equal to the difference between the frequencies of the injected signal (f_{in}) and the orthogonal mode of the VCSEL ($f_\perp$), of $\Delta f = f_{in} - f_\perp = -2.83 GHz$. The signal had perturbations with $t_d = 3.3$ ns and $k_p = 1.168$. Fig. 2(a) shows that at first the system is in a continuous (tonic) spiking state. This response is produced by the constant injection which (at that detuning) drives the VCSEL into a tonic spiking regime [30][45]. This is suppressed upon the perturbation's arrival (fig. 2(a)) due to the sudden increase in injection strength forcing the VCSEL to injection-lock to the input signal. Hence, switching from spiking to constant emission is obtained [37][38]. This inhibitory response is maintained until the perturbation is removed when it switches back to tonic spiking. The temporal map in Fig. 2(c) plots the VCSEL's response to the arrival of 200 identical perturbations. This two dimensional map is obtained taking as a folding parameter the repetition period of the perturbations (T = $1/f_{rep}$) [47]. In fig. 2(c), the spikes are indicated by yellow dots whilst a constant intensity is depicted in blue. Fig. 2(c) clearly shows the reproducibility of the spiking inhibition behavior with the same response obtained for all perturbations.

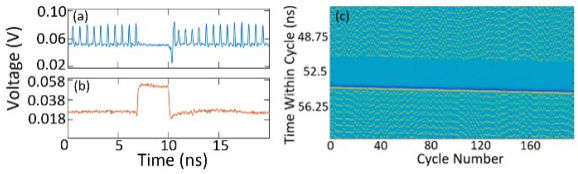

Fig. 2. Time series at the VCSEL's output (a) after the injection of the signal in (b) with a perturbation of t_d = 3.3 ns and k_p = 1.168. (c) Temporal map showing repeatable spiking inhibition for 200 perturbations entering the VCSEL. The rest of parameters are: I_{Bias} = 2mA; K_{inj} = 33.56 μW and Δf = -2.83 GHz.

Figs. 3(a-d) plot measured time series when the VCSEL is subject to the injection of signals with perturbations of different t_d, from *0* to *5.3 ns* (and constant $k_p = 1.168$). The rest of parameters are indicated in the figure caption. Fig. 3(a) shows that, without perturbations ($t_d = 0$) the VCSEL fires spikes with sub-ns intervals. Figs. 3(b-d) show in turn that when a perturbation is added the spiking dynamics are suppressed during the entire perturbation's time: 1.*89 ns* (fig. 3(b)), *3.3 ns* (fig. 3(c)) and *5.3 ns* (fig. 3(d)). Since t_d can be easily tuned experimentally, this offers a simple route for the controllability of the spike inhibition, much as inhibitory neurons do in the brain [43-45]. This is further illustrated in the map of fig. 3(e) merging results obtained for ten values of t_d from *0.89* to *9.82 ns*, plotting in each case the response to 20 perturbations.

Figs. 4(a-d) plot measured time-series in response to injected perturbations with constant duration ($t_d = 7.45$ *ns*) and varying strengths k_p from *0* to *0.803*. The rest of parameters are given in the figure caption. Fig. 4(a) plots first

the case where no perturbations are added and hence tonic spiking is obtained. Fig. 4(b) plots results when a small intensity perturbation (k_p = *0.219*) is added showing that tonic spiking is still obtained. However, during the perturbation higher amplitude spikes with longer spiking period are fired. When k_p = *0.516*, a similar response is seen (fig. 4(c)) obtaining a longer spiking period during the perturbation's time. Finally, for k_p = *0.803*, the VCSEL's spiking activity is fully inhibited. Thus, a threshold value of k_p has to be exceeded in order to obtain spike inhibition. The temporal map in fig. 4(e) merges results for five values of k_p plotting also the system's response to 40 perturbations in each case. Again, the results are reproducible with all perturbations yielding analogous responses. Fig. 4(e) also shows the controllability of the inhibition response which is only achieved for high enough values of k_p.

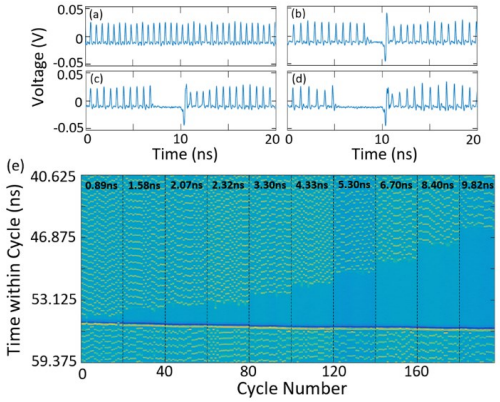

Fig. 3. (a-d) Time series and (e) temporal map of the VCSEL in response to perturbations with different t_d*: (a) 0, (b) 1.89, (c) 3.3, (d) 5.3 ns and constant* k_p *= 1.168. The map in (e) merges results for 20 perturbations for 10 different values of* t_d*. The other parameters are:* I_{Bias} *= 2mA;* K_{inj} *= 33.56 μW and Δf = -2.83 GHz.*

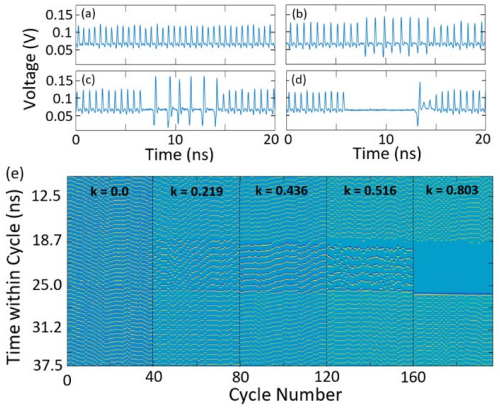

Fig. 4. (a)-(d) Time series and (e) temporal map of the VCSEL in response to perturbations with constant t_d *= 7.45 ns and different strength,* k_p*: (a) 0, (b) 0.219, (c) 0.516, (d) 0.803. The map in (e) merges results for 40 perturbations and for 5* k_p *values. The other parameters are:* I_{Bias} *= 2mA;* K_{inj} *= 35.81 μW and Δf = -2.77 GHz.*

The experiments can be explained with a simple model considering the evolution of the laser's phase relative to that of the optical injection $\Phi = \Phi_{laser} - \Phi_{inj}$. Assuming a strong damping of the relaxation oscillation and a weak amplitude optical injection field with small detuning, the equation governing the evolution of Φ reads

$$\dot{\Phi} = \frac{-dU}{d\Phi}, \quad U(\Phi) = -\Delta\Phi - Y(t)\sqrt{1+\alpha^2}cos(\Phi + u) \quad (1)$$

where Δ is the detuning between the laser's frequency and that of the optical injection with amplitude Y; α is the linewidth enhancement factor and $u = arctan\ \alpha$ (see [29]). For a steady value of Y, the system possesses a single stable (and an unstable) equilibrium point, provided that $Y \geq Y_c$, with $Y_c = |\Delta|/\sqrt{1+\alpha^2}$. In this case, the potential $U(\Phi)$ exhibits a minima and a maxima corresponding to these two fixed points, respectively. When the system is operated with $Y < Y_c$, the potential $U(\Phi)$ has no minima and Φ_{laser} is unlocked from Φ_{inj}. As such, Φ drifts non-linearly in a slanted "washboard" potential. Each time the VCSEL's frequency approaches that of ML, Φ remains for a long interval close to the position of the two annihilated fixed points, drifting then away more rapidly and performing a 2π rotation [30]. It is that excursion of Φ that yields an intensity spike. However, the monitored intensity is the superposition of the injected field reflected by the VCSEL's top mirror and that emitted by the device proportional to $I_{out} = |1 + ke^{i\Phi}|^2$. This coherent superposition of two fields is not trivial and depends critically on the proportionality coefficient k, which is a function of the pumping current and the reflectivities of the VCSEL's mirrors (see [29]). Small changes in facet reflectivities can modify k from 0.1 to 10 transforming into upward or downward the detected spikes. A good agreement was found for k = *-0.05*.

Fig. 5(a) depicts a situation where $Y < Y_c$ at all times except for three short intervals where $Y > Y_c$ (with different strength). This suppresses the tonic spiking behaviour for those time intervals as seen experimentally in figs. 3 and 4. Besides, fig. 5(a) shows that the exact injection's amplitude is not critical as long as it exceeds Y_c. Fig. 5(b) also shows that tuning the injection field's amplitude below Y_c allows the control of the inter-spiking interval, in agreement with the experiments in fig. 4. We should also note that Eq. (1) experiences a saddle-node bifurcation on an invariant circle (SNIC) when $Y = Y_c$ yielding a transition from a steady to a periodic behavior via a homoclinic bifurcation. The spiking period is directly proportional to the distance from the bifurcation point. Hence, tuning the distance from the SNIC allows to control the inhibitory response as needed for STPD algorithms [12]. Finally, we must note that the marked rebound spike after the injection field is lowered (see fig. 2 at t = *10ns*) is not observed here. This may be reproduced with a more complex model considering the population inversion and intensity dynamics and thus the relaxation oscillations. In that situation richer and more complex dynamics (e.g. multipulse excitability) are expected [48].

In summary, we demonstrate an inhibitory photonic neuronal model with a VCSEL showing high speeds (sub-ns operation) and low input power requirements (~tens of μWs). Reproducible spiking inhibition is achieved in response to perturbations encoded in injected signals. Moreover, full control of the spiking inhibition responses is

achieved by acting on the perturbation's duration and strength. These results obtained with off-the-shelve devices operating at telecom wavelengths, added to the unique attributes of VCSELs offer great prospects for their use as a single platform for photonic excitatory [30] and inhibitory neurons. We foresee that these will be key building blocks in future brain-inspired networks of photonic neurons for novel ultrafast neuromorphic computing systems.

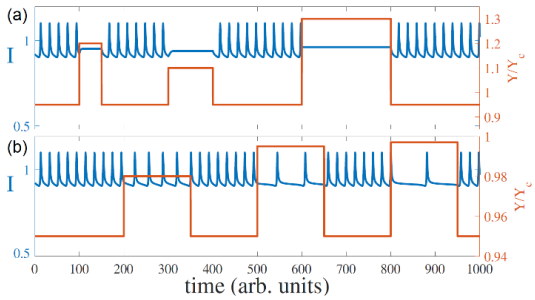

Fig. 5. Time traces for I (blue) and Y normalized to Y_c (orange). (a,b) The system operated in the unlocked regime ($Y = 0.95Y_c$) yielding tonic spiking. (a) For $Y>Y_c$ spiking is inhibited until the injection field is reduced. (b) Spiking period as a function of Y/Y_c. Other parameters are $\alpha=2$, $\Delta=-1$, such that $Y_c = 0.4472$.

Funding. University of Strathclyde (Chancellor's Fellowships Programme); Spanish Ministry of Education (Ramon y Cajal Programme project COMBINA (TEC2015-65212-C3-3-P AEI/FEDER UE); Chinese Scholarship Council (201506995013); National Natural Science Foundation of China (61674123).

Acknowledgment. AH wishes to thank Profs. T. Ackemann and A. Kemp for lending experimental equipment.

References

1. C. Mead, "Analogue VLSI and Neural Systems," Addison-Wesley (1989).
2. B. Benjamin, P. Gao, E. McQuinn, S. Choudhary, A. Chandrasekaran, J.-M. Bussat, R. Alvarez-Icaza, J. Arthur, P. Merolla, and K. Boahen, Proc. IEEE **102**, 699 (2014).
3. P. A. Merolla, J. V. Arthur, R. Alvarez-Icaza, A. S. Cassidy, J. Sawada, F. Akopyan, B. L. Jackson, N. Imam, C. Guo, Y. Nakamura, B. Brezzo, I. Vo, S. K. Esser, R. Appuswamy, B. Taba, A. Amir, M. D. Flickner, W. P. Risk, R. Manohar, and D. S. Modha, Science **345**, 668 (2014).
4. J. Schemmel, D. Briiderle, A. Griibl, M. Hock, K. Meier, and S. Millner, in Proc. of IEEE International Symposium on Circuits and Systems, 1947 (2010).
5. S. Furber, F. Galluppi, S. Temple, and L. Plana, Proc. IEEE **102**, 652 (2014).
6. P.R. Prucnal, B.J. Shastri, T. Ferreira de Lima, M.A. Nahmias and A.N. Tait, Adv. Opt. Photon., **8**, 228 (2016).
7. E.C. Mos, J.L. Hoppenbrouwers, M.T. Hill, M.W. Blüm, J.H.B. Schleipen, and H. de Waardt, IEEE Trans. Neural Netw. **11**, 988 (2000).
8. A.R.S. Romariz and K.H. Wagner, Appl. Opt., **48**, 4736 (2007).
9. A.R.S. Romariz and K.H. Wagner, Appl. Opt., **48**, 4746 (2007).
10. K. Kravtsov, M.P. Fok, D. Rosenbluth, and P.R. Prucnal, Opt. Exp. **19**, 2133 (2011).
11. M.P. Fok, Y. Tian, D. Rosenbluth and P.R. Prucnal, Opt. Letts. **37**, 3309 (2012).
12. R. Toole, A. N. Tait, T. Ferreira de Lima, M. A. Nahmias, B. J. Shastri, P. R. Prucnal, and M. P. Fok, J. Lightwave Technol., **34**, 470 (2016).
13. B.J. Shastri, M.A. Nahmias, A.N. Tait, B. Wu and P.R. Prucnal, Opt. Exp. **23**, 8029 (2015).
14. A.N. Tait, M.A. Nahmias, B.J. Shastri and P.R. Prucnal, J. Lightwave Technol. **32**, 3427 (2014).
15. B.J. Shastri, M.A. Nahmias, A.N. Tait and P.R. Prucnal, Opt. and Quantum Electron. **46**, 1353 (2014).
16. B.J. Shastri, M.A. Nahmias, A.N. Tait, A.W. Rodriguez, B. Wu and P.R. Prucnal, Sci. Rep. **6**, 19126 (2016)
17. A. M. Yacomotti, P. Monnier, F. Raineri, B. B. Bakir, C. Seassal, R. Raj, and J. A. Levenson, Phys. Rev. Letts. **97**, 143904 (2006).
18. M. Brunstein, A. M. Yacomotti, I. Sagnes, F. Raineri, L. Bigot, and A. Levenson, Phys. Rev. A **85**, 031803 (2012).
19. B. Romeira, J. Javaloyes, C.N. Ironside, J.M.L. Figueiredo, S. Balle, and O. Piro, Opt. Exp. **21**, 20931 (2013).
20. B. Romeira, R. Avo, J.M.L. Figueiredo, S. Barland and J. Javaloyes, Sci. Rep. **6**, 19510, (2016)
21. W. Coomans, L. Gelens, S. Beri, J. Danckaert, and G. Van der Sande, Phys. Rev. E. **84**, 036209 (2011).
22. M.A. Nahmias, B.J. Shastri, A.N. Tait and P.R. Prucnal, IEEE Journal of Sel. Top. Quantum Electron. **19**, 1800212 (2013).
23. S. Barbay, R. Kuszelewicz and A.M. Yacomotti, Opt. Letts. **36**, 4476 (2011).
24. F. Selmi, R. Braive, G. Beaudoin, I. Sagnes, R. Kuszelewicz, and S. Barbay, Phys. Rev. Letts. **112**, 183902 (2014).
25. F. Selmi, R. Braive, G. Beaudin, I. Sagnes, R. Kuszelewicz, T. Erneux and S. Barbay, Phys. Rev. E **94**, 042219 (2016)
26. A. Hurtado, I.D. Henning, and M.J. Adams, Opt. Exp. **18**, 25170 (2010).
27. A. Hurtado, K. Schires, I.D. Henning and M.J. Adams, Appl. Phys. Letts. **100**, 103703 (2012).
28. M. Turconi, B. Garbin, M. Feyereisen, M. Giudici and S. Barland, Phys. Rev. E **88**, 022923 (2013).
29. B. Garbin, J. Javaloyes, G. Tissoni and S. Barland, Nat. Commun., **6**, 5915 (2015).
30. A. Hurtado and J. Javaloyes, Appl. Phys. Letts., **107**, 241103 (2015)
31. J. Javaloyes, T. Ackemann and A. Hurtado, Phys. Rev. Letts. **115**, 203901 (2015).
32. D. Brunner, M. C. Soriano, C. R. Mirasso, and I. Fischer, Nat. Commun. **4**, 1364 (2013).
33. A. Aragoneses, S. Perrone, T. Sorrentino, M.C. Torrent and C. Masoller, Sci. Rep. **4**, 4696 (2014)
34. B. Kelleher, C. Bonatto, G. Huyet, and S. P. Hegarty, Phys. Rev. E **83**, 026207 (2011).
35. H.J. Wunsche, O. Brox, M. Radziunas, and F. Henneberger, Phys. Rev. Letts. **88**, 023901 (2002).
36. K. Al-Naimee, F. Marino, M. Ciszak, S. F. Abdalah, R. Meucci, and F. T. Arecchi, Eur. Phys. J. D **58**, 187 (2010).
37. S. Wieczorek, B. Krauskopf, T.B. Simpson, and D. Lenstra, Phys. Rep. **416**, 1 (2005).
38. A. Hurtado, A. Quirce, A. Valle, L. Pesquera, and M. J. Adams, Opt. Exp. **18**, 9423 (2010).
39. L.A. Coldren, S.W. Corzine and M.L. Mashanovitch, "Diode Lasers and Photonic Integrated Circuits," John Wiley & Sons, (2012).
40. F. Koyama, J. Lightwave Technol. **24**, 4502 (2006).
41. M.J. Adams, A. Hurtado, D. Labukhin and I.D. Henning, Chaos **20**, 037102 (2010).
42. E.M. Izhikevich, IEEE Trans. Neural Networks **15**, 1063 (2004).
43. E.M. Izhikevich, Int. J. Bifurcation and Chaos **10**, 1171 (2000)
44. E.R. Kandel, J.H. Schwartz, T.M. Jessell, "Principles of Neural Science", McGraw-Hill (2000)
45. I. Aldaya, C. Gosset, C. Wang, G. Campuzano, F. Grillot and G. Castañon, Electron. Letts. **51**, 280 (2015).
46. www.raycan.com
47. G. Giacomelli, F. Marino, M. A. Zaks and S. Yanchuk, Phys. Rev. E **88**, 062920 (2013).
48. S. Wieczorek, B. Krauskopf and D. Lenstra, Phys. Rev. Letts. **88**, 063901 (2002).

References

1. C. Mead, "Analogue VLSI and Neural Systems," Addison-Wesley (1989)
2. B. Benjamin, P. Gao, E. McQuinn, S. Choudhary, A. Chandrasekaran, J.-M. Bussat, R. Alvarez-Icaza, J. Arthur, P. Merolla, K. Boahen, "Neurogrid: A mixed-analog-digital multichip system for large-scale neural simulations," Proc. IEEE **102**, 699-716 (2014)
3. P.A. Merolla, J.V. Arthur, R. Alvarez-Icaza, A.S. Cassidy, J. Sawada, F. Akopyan, B.L. Jackson, N. Imam, C. Guo, Y. Nakamura, B. Brezzo, I. Vo, S.K. Esser, R. Appuswamy, B. Taba, A. Amir, M.D. Flickner, W.P. Risk, R. Manohar, D.S. Modha, "A million spiking-neuron integrated circuit with a scalable communication network and interface" Science **345**, 668-673 (2014)
4. J. Schemmel, D. Briiderle, A. Griibl, M. Hock, K. Meier, S. Millner, "A wafer-scale neuromorphic hardware system for large-scale neural modeling," Proc. of IEEE Int. Symp. Circuits and Systems, 1947-1950 (2010)
5. S. Furber, F. Galluppi, S. Temple, L. Plana, "The spinnaker project," Proc. IEEE **102**, 652-665 (2014)
6. P.R. Prucnal, B.J. Shastri, T. Ferreira de Lima, M.A. Nahmias A.N. Tait, "Recent progress in semiconductor excitable lasers for photonic spike processing," Adv. Opt. Photon., **8**, 228-299 (2016)
7. E.C. Mos, J.L. Hoppenbrouwers, M.T. Hill, M.W. Blüm, J.H.B. Schleipen, H. de Waardt, "Optical neuron by use of a laser diode with injection seeding and external optical feedback" IEEE Trans. Neural Netw. **11**, 988-996 (2000)
8. A.R.S. Romariz, K.H. Wagner, "Tunable vertical-cavity surface-emitting laser with feedback to implement a pulsed neural model. 1. Principles and experimental demonstration," Appl. Opt., **46**, 4736-4745 (2007).
9. A.R.S. Romariz, K.H. Wagner, "Tunable vertical-cavity surface-emitting laser with feedback to implement a pulsed neural model. 2. High-frequency effects and optical coupling," Appl. Opt., **48**, 4746-4753 (2007).
10. K. Kravtsov, M.P. Fok, D. Rosenbluth, P.R. Prucnal, "Ultrafast all-optical implementation of a leaky integrate-and-fire neuron," Opt. Exp. **19**, 2133-2147 (2011).
11. M.P. Fok, Y. Tian, D. Rosenbluth, P.R. Prucnal, "Asynchronous spiking photonic neuron for lightwave neuromorphic signal processing," Opt. Letts. **37**, 3309-3311 (2012).
12. R. Toole, A. N. Tait, T. Ferreira de Lima, M. A. Nahmias, B. J. Shastri, P. R. Prucnal, and M. P. Fok, "Photonic implementation of spike timing dependent plasticity and learning algorithms of biological neural systems," J. Lightwave Technol., **34**, 470–476 (2016).
13. B.J. Shastri, M.A. Nahmias, A.N. Tait, B. Wu, P.R. Prucnal, "Simpel: circuit model for photonic spike processing laser neuronsm" Opt. Exp. **23**, 8029-8044 (2015).
14. A.N. Tait, M.A. Nahmias, B.J. Shastri, P.R. Prucnal, "Broadcast and weight: an integrated network for scalable photonic spike processing," J. Lightwave Technol. **32**, 3427-3439 (2014).
15. B.J. Shastri, M.A. Nahmias, A.N. Tait, P.R. Prucnal, "Simulations of a graphene excitable laser for spike processing," Opt. and Quantum Electron. **46**, 1353-1358 (2014).
16. B.J. Shastri, M.A. Nahmias, A.N. Tait, A.W. Rodriguez, B. Wu, P.R. Prucnal "Spike processing with a graphene excitable laser,", Sci. Rep. **6**, 19126 (2016)
17. A.M. Yacomotti, P. Monnier, F. Raineri, B. B. Bakir, C. Seassal, R. Raj, J.A. Levenson, "Fast thermos-optical excitability in a two-dimensional photonic crystal," Phys. Rev. Letts. **97**, 143904 (2006).
18. M. Brunstein, A.M. Yacomotti, I. Sagnes, F. Raineri, L. Bigot, A. Levenson, "Excitability and self-pulsing in a photonic crystal nanocavity," Phys. Rev. A **85**, 031803 (2012).
19. B. Romeira, J. Javaloyes, C.N. Ironside, J.M.L. Figueiredo, S. Balle, O. Piro, "Excitability and optical pulse generation in semiconductor lasers driven by resonant tunneling diode photo-detectors," Opt. Exp. **21**, 20931-20940 (2013).
20. B. Romeira, R. Avo, J.M.L. Figueiredo, S. Barland, J. Javaloyes, "Regenerative memory in time-delayed neuromorphic photonic resonators," Sci. Rep. **6**, 19510 (2016)
21. W. Coomans, L. Gelens, S. Beri, J. Danckaert, G. Van der Sande, "Solitary and coupled semiconductor ring lasers as optical spiking neurons," Phys. Rev. E. **84**, 036209 (2011).
22. M.A. Nahmias, B.J. Shastri, A.N. Tait, P.R. Prucnal, "A Leaky Integrate-and-Fire Laser Neuron for Ultrafast Cognitive Computing," IEEE Journal of Sel. Top. Quantum Electron. **19**, 1-12 (2013).
23. S. Barbay, R. Kuszelewicz, A.M. Yacomotti, "Excitability in a semiconductor laser with saturable absorber," Opt. Letts. **36**, 4476-4478, (2011).
24. F. Selmi, R. Braive, G. Beaudoin, I. Sagnes, R. Kuszelewicz, S. Barbay, "Relative refractory period in an excitable semiconductor laser," Phys. Rev. Letts. **112**, 183902 (2014).
25. F. Selmi, R. Braive, G. Beaudin, I. Sagnes, R. Kuszelewicz, T. Erneux, S. Birbay, "Spike latency and response properties of an excitable micropillar laser," Phys. Rev. E **94**, 042219 (2016)
26. A. Hurtado, I.D. Henning, M.J. Adams, "Optical neuron using polarisation switching in a 1550nm-VCSEL," Opt. Exp. **18**, 25170-25176 (2010).
27. A. Hurtado, K. Schires, I.D. Henning, M.J. Adams, "Investigation of vertical cavity surface emitting laser dynamics for neuromorphic photonic systems," Appl. Phys. Letts. **100**, 103703 (2012).
28. M. Turconi, B. Garbin, M. Feyereisen, M. Giudici, S. Barland, "Control of excitable pulses in an injection-locked semiconductor laser," Phys. Rev. E **88**, 022923 (2013).
29. B. Garbin, J. Javaloyes, G. Tissoni, S. Barland, "Topological solitons as addressable phase bits in a driven laser," Nat. Commun., **6**, 5915 (2015).
30. A. Hurtado, J. Javaloyes, "Controllable spiking patterns in long-wavelength vertical cavity surface emitting lasers for neuromorphic photonic systems," Appl. Phys. Letts., **107**, 241103 (2015)
31. J. Javaloyes, T. Ackemann, A. Hurtado, "Arrest of domain coarsening via antiperiodic regimes in delay systems," Phys. Rev. Lett. **115**, 203901 (2015).
32. D. Brunner, M. C. Soriano, C. R. Mirasso, I. Fischer, "Parallel photonic information processing at gigabyte per second data rates using transient states," Nat. Commun. **4**, 1364 (2013).
33. A. Aragoneses, S. Perrone, T. Sorrentino, M.C. Torrent, C. Masoller, "Unveiling the complex organization of recurrent patterns in spiking dynamical systems," Sci. Rep. **4**, 4696 (2014)
34. B. Kelleher, C. Bonatto, G. Huyet, S. P. Hegarty, "Excitability in optically injected semiconductor lasers: contrasting quantum-well and quantum-dot-based devices," Phys. Rev. E **83**, 026207 (2011).
35. H.J. Wunsche, O. Brox, M. Radziunas, F. Henneberger, "Excitability of a Semiconductor Laser by a Two-Mode Homoclinic Bifurcation," Phys. Rev. Letts. **88**, 023901 (2002).
36. K. Al-Naimee, F. Marino, M. Ciszak, S.F. Abdalah, R. Meucci, F.T. Arecchi, "Excitability of periodic and chaotic attractors in semiconductor lasers with optoelectronic feedback" Eur. Phys. J. D **58**, 187-189 (2010)
37. S. Wieczorek, B. Krauskopf, T.B. Simpson, D. Lenstra, "The dynamical complexity of optically injected semiconductor lasers," Phys. Rep. **416**, 1 (2005).
38. A. Hurtado, A. Quirce, A. Valle, L. Pesquera, M. J. Adams, "Nonlinear dynamics induced by parallel and orthogonal optical injection in 1550 nm vertical-cavity surface-emitting lasers (VCSELs)," Opt. Exp. **18**, 9423 (2010)
39. L.A. Coldren, S.W. Corzine, M.L. Mashanovitch, "Diode Lasers and Photonic Integrated Circuits," John Wiley & Sons, (2012)
40. F. Koyama, "Recent advances of VCSEL photonics," J. Lightwave Technol. **24**, 4502-4513 (2006)
41. M.J. Adams, A. Hurtado, D. Labukhin, I.D. Henning, "Nonlinear semiconductor lasers and amplifiers for all-optical information processing," Chaos **20**, 037102 (2010)
42. E.M. Izhikevich, "Which model to use for cortical spiking neurons?," IEEE Trans. Neural Networks **15**, 1063-1070 (2004)
43. E.M. Izhikevich, "Neural excitability, spiking and bursting" Int. J. Bifurcation and Chaos **10**, 1171 (2000)
44. E.R. Kandel, J.H. Schwartz, T.M. Jessell, "Principles of Neural Science", McGraw-Hill (2000)

45. I. Aldaya, C. Gosset, C. Wang, G. Campuzano, F. Grillot, G. Castañon, "Periodic and aperiodic pulse generation using optically injected DFB laser," Electron. Letts. **51**, 280 (2015)
46. www.raycan.com
47. G. Giacomelli, F. Marino, M.A. Zaks, S. Yanchuk, "Nucleation in bistable dynamical systems with long delay," Phys. Rev. E **88**, 062920 (2013)
48. S. Wieczorek, B. Krauskopf and D. Lenstra, "Multipulse excitability in a semiconductor laser with optical injection," Phys. Rev. Letts. **88**, 063901 (2002).